Int. J. Nanosci. Nanotechnol., Vol. 8, No. 3, Sep. 2012, pp. 127-134

Ultra-Sharpening of Diamond Stylus by 500 eV O^+/O_2^+ Ion Beam Machining without Facet and Ripple Formation

S. F. Mahmud[1,2,*], J. Taniguchi

1- Department of Applied Electronics, Tokyo University of Science, Japan
2- Bangabandhu Fellowship on ICT Project, Bangladesh

(*) Corresponding author: sf.mahmud19@yahoo.com
(Received:02 Jul. 2012 and Accepted: 28 Sep. 2012)

Abstract:
The price of single point diamond tools with a sharp tip is very high due to complex machining process and highly expensive machining equipments. Yet, the performance is not quite satisfactory. In this paper, we have presented a very simple and cost effective machining process for the sharpening and polishing of diamond stylus using low energy reactive ion beam machining (RIBM). In our method, machining of the stylus was done by 500 eV O^+/O_2^+ ion beam at an off-normal ion incidence angle under rotating condition. Mechanically coarse-finished styli of two different size and shape were used as the specimen- stylus of apex angle 90° with the radius of curvature 5μm and stylus of apex angle 60° with the radius of curvature 2μm. In both cases, the stylus was sharpened down to an apex angle of around 55° with the radius of curvature ≤100 nm. The tilt angle of the specimen for shrapening was predicted from simulation. The surface of the processed stylus was completely smooth and ripple-free and the surface defects on the pristine stylus were also eliminated by the proposed machining method. Due to low energy RIBM, the irradiation damage on the diamond crystalline structure was minimal.
Keywords: *Ultera-sharpening, Diamond, Ion Beam Machine.*

1. INTRODUCTION

Owing to supreme hardness and tensile strength and high wear resistance, diamond is used as a source material in many electro-mechanical devices. Diamond tips are used as probes and styli for large area profile measurement, repeated scanning, photo mask repairing, scanning force microscopy lithography and magnetic force microscopy (Magnetic material coated diamond probe) lithography. Diamond stylus is also used as scriber for dicing on semiconductor wafers, substrates and LCDs. In order to ensure narrow and deep scribing line without adverse impact on the wafers, a conical shaped diamond stylus with smooth and sharp tip is highly desirable. The apex angle of most commonly found diamond stylus is 90°-110° with the curvature radius of 5μm. A commercially available 60° diamond stylus with a curvature radius of 2μm is highly expensive due to complex and costly manufacturing. Moreover, most of the 60° styli possess surface deffects in the tip area which limits their performance with high accuracy. Therefore, a feasible and cost effective machining procedure for the fabrication of smooth and sharp conical shaped diamond stylus with sub-micron sized tip radius is yet a challenge.

Usually, diamond tools such as single-point tools, styli and indenters are processed by a mechanical polishing step.These polishing techniques generally use a diamond fine powder and a lap board made from cast iron. However, these particular mechanical processes cause micro-chipping at the edge and therefore, cannot be extended to form finer and

sharper tips. Compared to mechanical processing, dry etching processes, such as PE (plasma etching) [1], RIE (reactive ion etching) [2-3], IBM (ion beam machining) [4-6], RIBM (reactive ion beam machining) [6] and FIB (focused ion beam) machining are more effective for the ultra-fine processing of super hard and brittle materials such as diamond. RIE cannot be suitably applied for the sharpening of diamond probes since in this method, the incident angle of the ions cannot be changed as required, and hence it becomes difficult to control the shape of the diamond tip. FIB machining method is most commonly applied for the sharpening of diamond probe [7], and for forming of diamond micro-tools [8-9].

However, this process also has some substantial drawbacks such as formation of ripples on the probe's surface, high irradiation damage (due to high operating energy, usually about 40-50 keV) and high machining cost. The limitations of FIB machining can be eliminated to a great extent by broad ion beam machining (BIBM) of the diamond tools at comparatively lower ion energy (0.3 keV-10 keV). In BIBM, the diamond tools are usually sharpened at normal incidence angles and the sharpening conditions are predicted by the Witcomb formula [10]. According to Witcomb formula, higher ion energy is required for higher sharpness of the tip and on the other hand, facet will be formed at the tip if machining is done at very low ion energy. Therefore, in most cases of IBM, the ion energy is in the range of 3-10 keV to get a sharp diamond tip of apex angle $\leq 60°$. In this range of ion energy, the irradiation damage of the diamond surface becomes significant and machine equipments are also expensive. In addition to this, ripples are formed on the surface of the diamond tools. Miyamoto *et al.* discussed several examples of forming and sharpening of diamond tools by ion beam combined with mechanical pre-finishing [11].

However, in these methods the apex angle of the tools remained unchanged. Moreover, there was no discussion regarding the formation of ripple on the processed tip and how to check the formation of ripple. We developed 1 keV Ar^+ ion beam machining to form a shell-type diamond stylus from a conical shaped stylus by swinging it about the axis of ion beam irradiation [12]. But in this case, the shape of the stylus changes and hence cannot be applied to form a sharp conical shaped stylus.

In order to overcome the above limitations, we proposed reactive ion beam machining (RIBM) for the sharpening and polishing of mechanically pre-finished diamond stylus. Compared to IBM, RIBM ensures much lower irradiation damage on the diamond crystalline structure due to beneficial contribution of chemical sputtering [13]. Moreover, the etching rate is significantly higher for RIBM at low ion energy than the IBM.

In order to avoid facet formation at the tip, the stylus was machined at off-normal incidence angle and to retain the conical shape, the stylus was rotated around its own axis during the ion beam irradiation. We also developed a simulation model for predicting the tilt angle of the specimen for maximum sharpening. After 7 hours of machining, the diamond stylus of apex angle 90° with the tip radius of 5 μm was sharpened to an apex angle of 55° with only 100 nm radius of curvature. Almost the same result was observed when a 60° stylus with the radius of curvature 2 μm was processed in the same manner. Furthermore, the surface of the processed stylus was completely smooth and ripple free.

Our proposed method is unique in the sense that this is first ever approach of sharpening diamond micro-styli of different size and shape by using low energy RIBM and this method eliminates most of the major drawbacks of IBM and FIB machining.

2. EXPERIMENTAL APPARATUS

The experiments were conducted in an electron cyclotron resonance (ECR) type ion beam apparatus which can generate broad oxygen ion beam in the energy range of 0.3-3 keV. The pressure inside the plasma generation chamber was set at 1×10^{-4} Pa. Oxygen gas was passed into the plasma generation chamber, ion was formed inside the chamber and then the diamond styli were sputtered at off-normal incidence angle under rotating condition. The tilt angle for off-normal incidence sputtering was predicted by the simulation model developed

using Matlab software. The measurement of etching depth of natural single crystal diamond chip (100) was done by Alpha-Step 500 surface profiler. The un-processed and processed diamond styli were observed by a scanning electron microscope (SEM) to realize the profile change due to ion beam irradiation.

3. RESULTS AND DISCUSSION

3.1. Etching rate calculation

In order to achieve high machining speed of processing the stylus, we at first measured the etching rate of diamond on a flat diamond surface by O^+/O_2^+ ion beam machining at the ion energy 0.3 ~ 3 keV. It was found that the ion current density decreased from 1.2 mA/cm^2 to 0.6 mA/cm^2 as the ion energy was decreased from 3 keV to 0.3 keV. Figure 1(a) shows the plot of etching rate vs. ion energy for O^+/O_2^+ ion beam at normal ion incidence. As shown in Figure 1(a), the etching rate, V was the highest at 500 eV ion energy at the ion current density, i= 1.06 mA/cm^2 within the range of ion energy, E= 0.3 ~3 keV. Figure 1(b) shows the dependence of etching rate, V on ion incidence angle, θ for 500 eV O^+/O_2^+ ion beam machining. From Figure 1(b), it is apparent that the etching rate decreases with increasing the angle of ion incidence and the maximum etching rate was obtained at normal angle of ion incidence. During the oxygen ion beam etching process, both chemical and physical sputtering take place. The proportion of chemical sputtering and physical sputtering depends on the ion energy and ion incidence angle. At 300 eV ion energy, the etching of diamond mainly occurs by the reaction between the target atoms and ions at the subsurface of the target and the contribution of physical sputtering is almost negligible. However, the physical sputtering becomes more prominent at high energy.

When the ion energy exceeds 500 eV, oxygen ions are absorbed on the diamond chip and therefore, carbon atoms are etched out by physical sputtering rather than chemical reaction with oxygen. Therefore, the etching rate starts decreasing with increasing ion energy.

3.2. Simulation for the prediction of profile change

The simulation of the profile change by 500 eV O^+/O_2^+ ion beam machining was done for both types of styli (stylus-1: apex angle 90°, radius of curvature 5 µm and stlus-2: apex angle 60° and radius of curvature 2 µm). Due to hemispherical shape of the tip, the ion incidence angle on each segment of the stylus will be different and hence the etching rate. Now we consider an initial point $P_0(x_{0'}, y_{0'}, z_{0'})$ on the curved surface of the stylus as shown in Figure 2. The ion incidence angle at P_0 is $\phi_{0'}$. When the stylus is tilted at an angle β towards

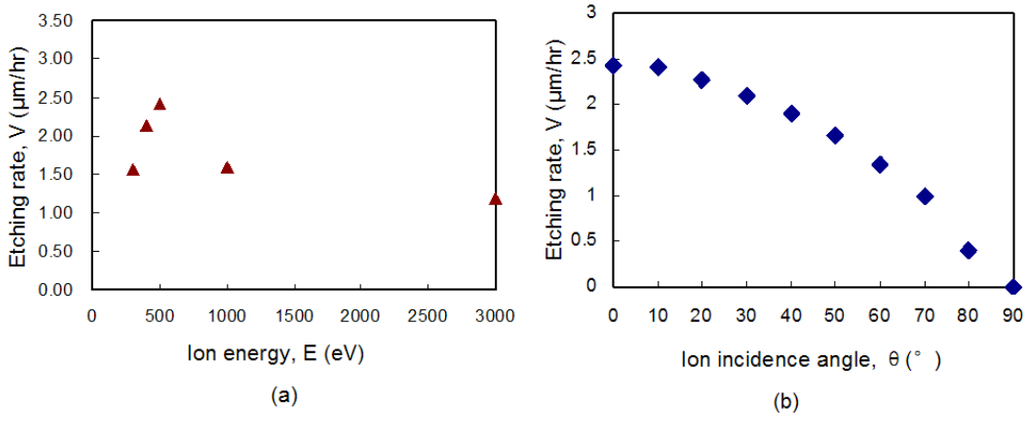

Figure 1: *Dependence of the etching rate of natural single crystal diamond (100) on (a) O^+/O_2^+ ion energy at normal incidence (θ=0°) b) ion incidence angle of 500 eV O^+/O_2^+ ion beam at the ion current density, i= 1.06 mA/cm^2*

the x axis, the ion incidence angle in the X-Y plane at point $P_0(x_0, y_0)$ would be $\phi = \beta - \phi_0$. $V(\phi)$ is the etching rate corresponding to ϕ. Due to ion beam machining for t hours, the point $P_0(x_0, y_0)$ will move to a new point $P(x, y)$ which can be expressed by the following equations according to Ducommun *et al.* [14] for the X-Y plane -

$$x = x_0 - \left\{ \frac{dV(\phi)}{d\phi} \cos\phi + V(\phi) \sin\phi \right\} t \qquad (1)$$

$$y = y_0 + \left\{ \frac{dV(\phi)}{d\phi} \sin\phi - V(\phi) \cos\phi \right\} t \qquad (2)$$

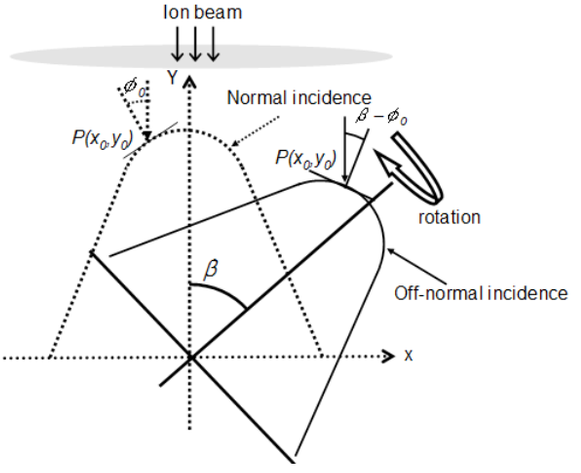

Figure 2: *Schematic diagram of sharpening diamond stylus. The diagram with dotted line represents irradiation on the stylus at normal incidence and the diagram with solid lines represents irradiation at off-normal incidence where the stylus is tilted at an angle β and rotated around its own axis.*

Now, when the stylus is rotated by an angle of 90° around its own axis, the incident ions at P_0 will have a shadowing effect. We may assume that the etching rate at P_0 would have a Gaussian distribution of $V(\phi)$ in one half of the rotation cycle and in the other half-cycle, the etching rate will be zero. Therefore, the average etching rate per rotation may be considered $Va = V(\phi)/4$. Due to rotation, the profile change of the stylus will be symmetrical in the X-Y and Y-Z plane and can be predicted from equations (1) and (2) except that $V(\phi)$ will be replaced by Va.

Figure 3 shows the profile change of 90° diamond stylus obtained from simulation due to 500 eV O^+/O_2^+ ion beam machining. As shown in Figure 3(a), when the tilt angle, β=40°, the stylus becomes blunt and facet is formed. When β is increased to 50°, the stylus becomes sharp without facet formation and the stylus becomes sharper when β is increased further to 70°.

Figure 4 represents the profile change of the diamond stylus of apex angle 60° and tip radius of 2 µm due to 500 eV O^+/O_2^+ ion beam machining. In this case for β=50°, the stylus is sharpened accompanying facet formation at the tip as shown in Figure 4(b). However, sharpening of the stylus is achieved without facet formation when β is increased to 70° which is shown in Figure 4(b). From Figure 4(c) it appears that the stylus can be sharpened further maintaining a high aspect ratio when β is increased to 90°.

Therefore, it is apparent from Figs. 3 and 4 that there is a minimum tilt angle for the stylus to get sharpening without facet formation. The minimum tilt angles, β_{min} is 50° and 70° for the styli of apex angle of 90° and 60° respectively and in both cases the sharpness of the stylus increases with increasing the tilt angle.

3.3. Experimental observation

Figure 5(a) shows the SEM image of an unprocessed diamond stylus of apex angle of 90° and radius of curvature of 5 µm. Figure 5(b) shows the SEM image of the same stylus after machining for 3 hours by the 500 eV O^+/O_2^+ ion beam at the tilt angle of 40°. As predicted by the simulation, the tip of the stylus became blunt forming a facet angle of 105° due to the machining at the tilt angle of 40°.

Figure 6(a) shows the SEM image of another unprocessed diamond stylus (apex angle 90°) with radius of curvature 5 µm that was subjected to 500 eV O^+/O_2^+ ion beam machining at the tilt angle of 70°. Figures 6(b) and (c) show the images of the processed stylus after machining for 1.5 hour and 3 hours, respectively. As predicted by the simulation, the sharpness of the stylus increases with machining time. The image of the processed stylus after 7 hours of machining is shown in Figure 6(d). As shown in the figure, the tip of the stylus

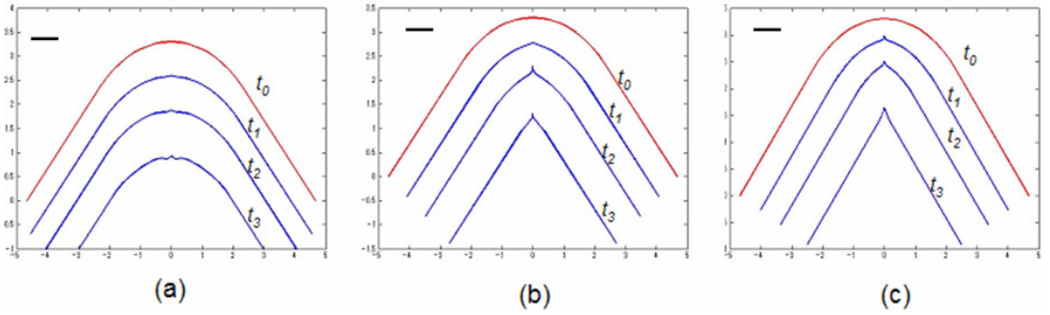

Figure 3: *Simulation of the profile change of diamond stylus with an apex angle, α = 90° and radius of curvature, r= 5 μm due to 500 eV O^+/O_2^+ ion beam machining (a) at β=40°, (b) β =50°, (c) β =70°. t_0 is the initial time, t_1, t_2, t_3 are the machining duration ($t_1 < t_2 < t_3$). The scale bar indicates 1 μm*

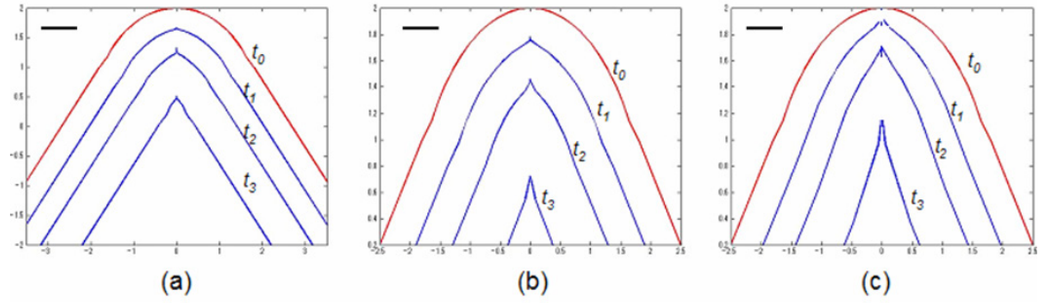

Figure 4: *Simulation of the profile change of diamond stylus with an apex angle, α =60° and radius of curvature, r= 2 μm due to 500 eV O^+/O_2^+ ion beam machining (a) at β =50°, (b) β =70°, (c) β =90°. t_0 is the initial time, t_1, t_2, t_3 are the machining duration ($t_1 < t_2 < t_3$). The scale bar indicates 1 μm*

became very sharp with an apex angle of 56° and the radius of curvature of the tip reduced down from 5 μm to only 100 nm due to machining for 7 hours at the tilt angle of 70°. Moreover, no ripple was observed on the processed tip.

Figure 7(a) shows the SEM image of a stylus (apex angle 60°) with radius of curvature 2 μm, Figure 7(b) shows the zoom-in image of the tip area. It is quite clear from Figure 7(b) that the surface condition in the tip area is very poor with many defects and protrusions. Though the price of a commercially available 60° diamond stylus is usually 4 times higher than that of a 90° stylus, most of the 60° stylus contain surface defects at the tip and hence they are not suitable for high precision measurements or performance. Figure 7(c) shows the image of the processed stylus after machining for 6 hours at the tilt angle of 90° by 500 eV O^+/O_2^+ ion beam. The apex angle of the processed stylus was 54° with the radius of curvature <100 nm. Figure 7(d) shows the zoom-in image of the processed stylus. It is quite obvious from Figure 7(d) that all the protrusions and surface irregularities present on the pristine stylus were eliminated due to proposed machining by 500 eV O^+/O_2^+ ion beam and the surface of the processed stylus became completely smooth and ripple-free. The reason of surface smoothening as observed in our experiments is discussed in the next section.

3.4. Surface smoothening and elimination of surface defects

In the final stage of processing of the diamond stylus, the ion incidence angle, θ on the tip was ≥50°. Generally ripples are formed on diamond surface at ion incidence angle of θ= 50°-70° [15], though in our case surface of stylus appeared smooth and ripple-free. The reason of suppressing

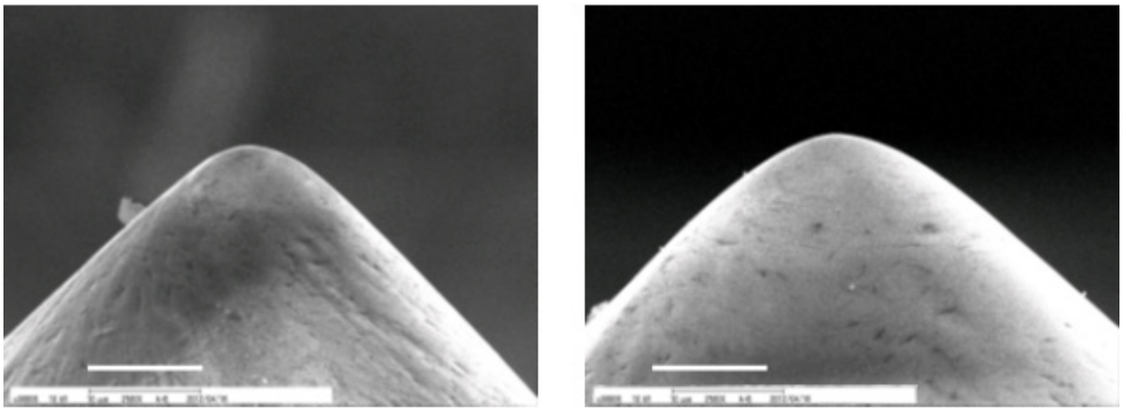

Figure 5: *SEM images of a diamond stylus of apex angle 90° and radius of curvature 5 µm (a) before processing (b) after processing by 500 eV O^+/O_2^+ ion beam for 3 hours at β =40°. The scale bar indicates 10 µm.*

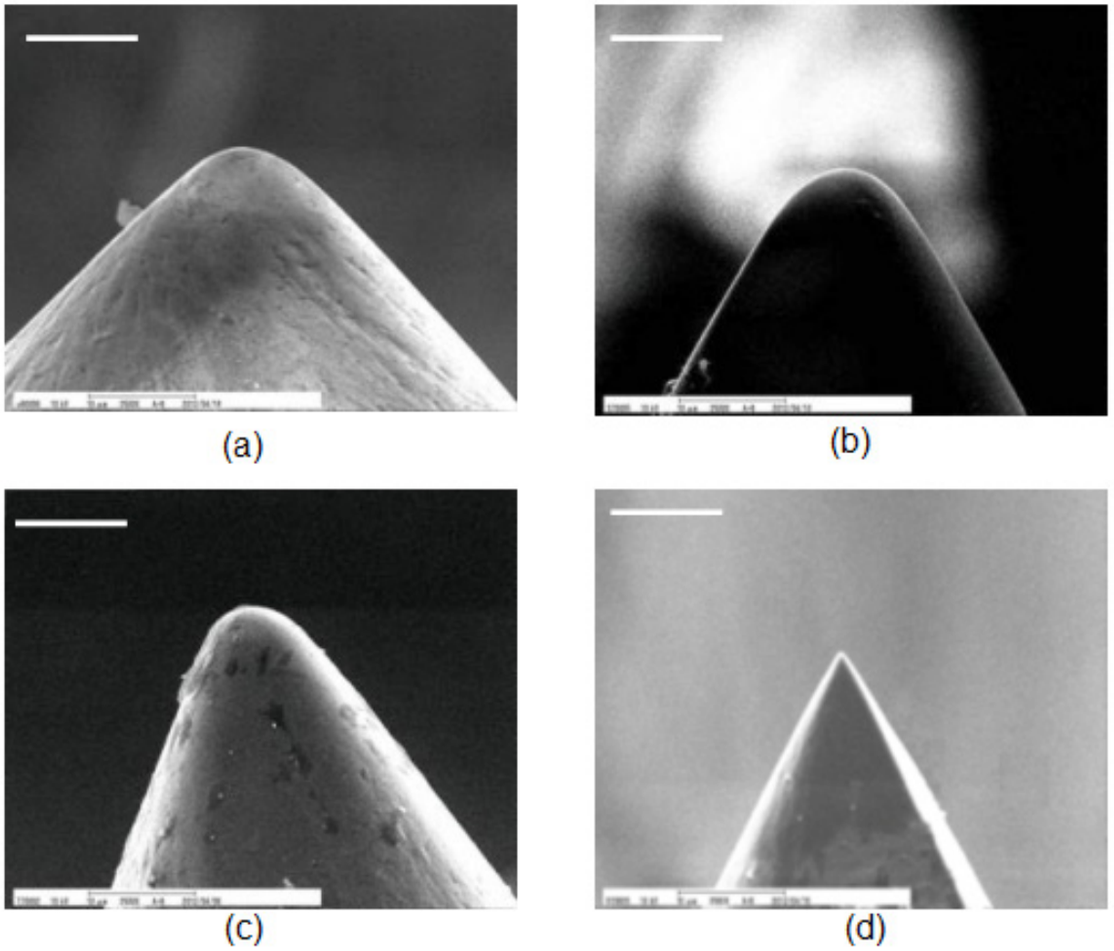

Figure 6: *SEM images of a diamond stylus of apex angle 90°and radius of curvature 5 µm (a) before processing, after processing by 500 eV O^+/O_2^+ ion beam at β =70° (b) for 1.5 hour, (b) for 3 hours (b) for 7 hours. The scale bar indicates 10 µm.*

ripple formation may be ascribed to rotation of the sample during machining. According to Bradley and Cirlin *et al*. [16, 17], when the sample is rotated, the smoothening effects of viscous flow and surface self-diffusion may prevail over the roughening effect of the curvature-dependent sputter yield and generate a smooth surface. Secondly, the reason of surface smoothening at region very near the tip may be attributed to enhanced erosion of the surface protrusions at the grazing incidence (θ>70°).

Usually at grazing incidence, most of the incident ions will be reflected away after collisions with surface atoms. This situation changes if the ion impinges near surface steps or similar surface irregularities, where the probability of sputtering off atoms from the surface is significantly increased [18]. Moreover, grazing incidence on the surface is equivalent to near normal incidence on the surface protrusions. As observed in our experiment (Figure 1), chemical sputtering is stronger towards lower ion energy and normal incidence. Therefore, in case of 500 eV O^+/O_2^+ beam machining, the protrusions and defects on the surface of the tip were etched out by the chemical sputtering effect of the O^+/O_2^+ ion leading the surface become smooth. The smoothening effect was enhanced due to machining under rotating condition.

3.5. Irradiation damage by IBM

Another significant factor need to account during IBM is the irradiation damage. When a diamond surface is bombarded by ion beam, a damage layer is induced by the physical sputtering and the diamond crystal structure changes into amorphous carbon or graphite. Physical sputtering becomes more pronounced as the ion energy increases which causes higher irradiation damage. Kawabata *et al*. identified the irradiation damage of different ion

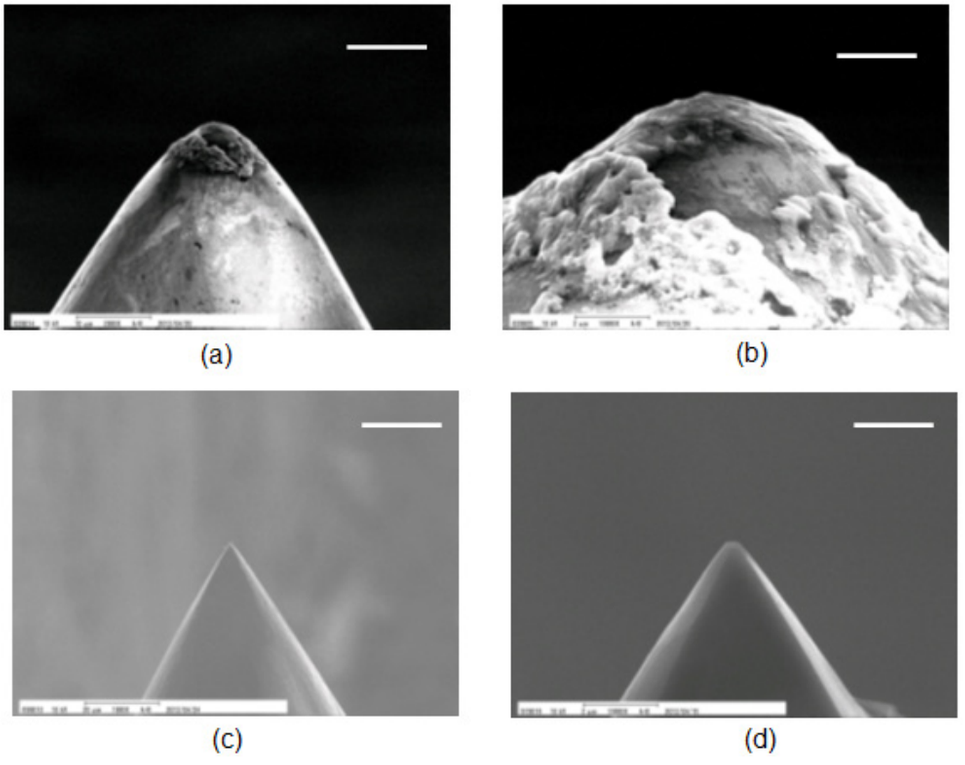

Figure 7: *SEM images of a diamond stylus of apex angle 60° and radius of curvature 2 µm (a) before processing, (b) zoom-in image of the tip before processing, (c) after processing for 6 hours with the apex angle 54° (d) zoom-in image of the tip after processing for 6 hours by 500 eV O^+/O_2^+ ion beam at β =90°. The scale bars in Figures(a) and (c) indicate 10 µm and in Figures(b) and (d) indicate 2 µm.*

beam etching process by the shift of binding energy from 285.2 (diamond) to 284.2 (graphite) and broadening of the peak in the XPS profile [13].
They reported that RIBAE and RIBM have lower tendency to form graphite than IBE and IBAE. It is because in RIBAE and RIBM, chemical sputtering takes a significant role and it becomes more pronounced towards lower ion energy. The pronounced contribution of chemical sputtering in the etching process by 500 eV O^+/O_2^+ ion beam was also evident during our experiment on the measurement of etching rate (Figure 1(a)). Therefore, in case of oxygen ion beam processing, the physical sputtering induced damage structure on the diamond surface is simultaneously etched out by the chemical sputtering creating volatile substances like CO_2 or CO. Hence, the diamond composed base layer is mostly recovered by the RIBM.

4. CONCLUSION

In this paper, we have presented a very simple and cost effective machining process for the sharpening and ultra-smooth finishing of diamond stylus using low energy RIBM. By our proposed method, the diamond stylus of apex angle 90° with the radius of curvature 5μm and stylus of apex angle 60° with the curvature radius of 2μm became ultra sharp with the apex angle of around 55° and the curvature radius of ≤100 nm. A simulation model was developed to decide the tilt angle of the specimen during shrapening process. It was found that there is a minimum tilt angle for shrapening without facet formation and the sharpeness of the stylus increases as the tilt angle increases.
The surface of the processed stylus was completely smooth and rippl-free and the surface defects on the pristine stylus were also eliminated by the machining. Moreover, minimal irradiation damage on the diamond crystal structure was ensured in our proposed method by implementing low energy RIBM. Due to simplicity, low cost and better performance than all conventioanl methods of processing diamond tools, our proposed method will open the door of using diamond tools in a wide scale in probe based lithography and ultra-precision measurements.

REFERENCES

1. D. T. Tran, T. A. Grotjohn, D. K. Reinhard and J. Asmussen, Diamond and Relat. Mater. Vol. 17, (2008), p. 717.
2. M. D. Stoikou, P. John and J. I. B Wilson, Diamond and Relat. Mater. Vol. 17, (2008), pp. 1164-1168.
3. Y. Ando, Y. Nishibayashi, K. Kobashi, T. Hirao and K. Oura, Diamond and Relat. Mater. Vol. 11, (2002), pp. 824-827.
4. I. Miyamoto, Prec. Eng. Vol. 9, No. 2, (1987), pp. 71-78.
5. I. Miyamoto, J. Taniguchi and S. Kiyohara, New Diamond and Frontier Carbon Technol. Vol. 10, (2000), pp. 63-77.
6. T. J. Whetten, A. A. Armstead, T. A. Gizybowski and A. L. Ruoff, J. Vac. Sci. Technol. A, Vol. 2, No. 2, (1984), pp. 477-480.
7. A. Olbrich, B. Ebersberger, C. Boit, P. Niedermann and W. Hänni, J. Vac. Sci. Technol. B, Vol. 17, No. 4, (1999), pp. 1570-1574.
8. D. P. Adams, M. J. Vasile, T. M. Mayer and V. C. Hodges, J. Vac. Sci. Technol. B, Vol. 21, No. 6, (2003), pp. 2334-2343.
9. Y. N. Picard, D. P. Adams, M. J. Vasile and M. B. Ritchey, Prec. Eng. Vol. 27, (2003), pp. 59-69.
10. M. J. Witcomb, J. Mater. Sci. Vol. 9, (1974), pp. 551-563.
11. I. Miyamoto, Precis. Eng. Vol. 9, (1987), pp. 71-78.
12. S. F. Mahmud, R. Fukuyama, S.A. Pahlovy, I. Miyamoto, Diamond & Related Materials, Vol. 24, (2012), pp. 139–145.
13. Y. Kawabata, J. Taniguchi and I. Miyamoto, Diamond and Relat. Mater., Vol. 13, (2004), pp. 93–98.
14. J. P. Ducommun, M. Cantagrel and M. Marchal, J. Mater. Sci., Vol. 9, (1974), pp. 725-736.
15. S. F. Mahmud, S. A. Pahlovy, Y. Sato and I. Miyamoto, Diamond and Relat. Mater., Vol. 20, (2011), pp. 1056–1060.
16. R. M. Bradley and E-H Cirlin, Appl. Phys. Lett., Vol. 68, (1996), pp. 3722-3724.
17. R. M. Bradley, Phys. Rev. E, Vol. 54, (1996), pp. 6149-6153.
18. F. Frost, R. Fechner, B. Ziberi, J. Vollner, D. Flamm and A. Schimdler, J. Phys.: Condens. Matter, Vol. 21, (2009), pp. 224026-224045.